JOURNAL OF Materials CHEMISTRY

# Exercising control over the influence of the lattice misfit on the structure of oxide–oxide thin film interfaces

**Dean C. Sayle,[a] S. Andrada Maicaneanu,[a] Ben Slater[b] and C. Richard A. Catlow[b]**

[a]*Department of Environmental and Ordnance Systems, Cranfield University, Royal Military College of Science, Shrivenham, Swindon, UK SN6 8LA. E-mail: sayle@rmcs.cranfield.ac.uk*
[b]*The Royal Institution of Great Britain, 21 Albemarle Street, London, UK W1X 4BS*

***Received 2nd July 1999, Accepted 26th August 1999***

Thin film oxide–oxide interfaces with associated lattice misfits ranging from −20 to +27%, have been 'grown' by depositing ions onto a surface in conjunction with dynamics simulation and energy minimisation. Inspection of the resulting interfaces revealed significant structural features within the thin film. These included, for the CaO/MgO(100) system (+13% misfit), the exposure of various CaO surfaces at the interface; grain-boundary formation; the evolution of periodic arrays of misfit induced dislocations; lattice slip, and rotations of the thin film with respect to the support. In each case the driving force to such behaviour was attributed to the reduction in the strain energy generated within the interface which arises from the lattice misfit between the two materials. The implications of employing periodic boundary conditions within interface calculations are also addressed. For those interfaces with high associated lattice misfits: BaO/MgO (+27%), SrO/MgO (+20%) and MgO/SrO (−20%), the deposition procedure yielded thin films with amorphous type structures. In the second part of this study we have explored briefly how one may exercise a degree of control over the influence of the lattice misfit and its implications for the structure and consequently the chemical and physical properties of the thin film. For example, for the SrO/MgO system, by including a CaO buffer layer between the SrO thin film and the MgO support material, it was possible to generate a more coherent and crystalline thin film, contrasting to the amorphous type structures observed without the inclusion of a buffer layer. An alternative approach, in which dopant ions were introduced into the thin film, resulted in pseudomorphic growth. In particular, the dopant ions modified the lattice parameter of the thin film to be commensurate with that of the support.

## Introduction

The presence of an interface may influence profoundly the physical and chemical properties of a material. Such a phenomenon has been extensively exploited in many applications including catalysis, sensors, high-density recording media, solar cells and electronic applications. For example $V_2O_5$, when supported on $TiO_2$ exhibits catalytic activity, which is not observed for either the unsupported $V_2O_5$ nor the $TiO_2$ substrate.[1] Conversely, the influence of the interface may be deleterious, for example, when the superconducting material Y–Ba–Cu–O is supported on an MgO substrate, the misfit between the two materials is accommodated by the presence of grain-boundaries, dislocations and defects,[2] which degrade the electrical properties of the Y–Ba–Cu–O thin film. Much research has therefore been directed into gaining a better understanding of how the presence of an interface can lead to such changes and moreover, how such phenomena can be exploited to aid the fabrication of improved new materials with optimum properties.

In previous studies, a Near Coincidence Site Lattice (NCSL) theory,[3,4] which is based on geometrical criteria, was employed, in conjunction with energy minimisation, to generate interface structures with low associated misfits.[5] In particular, the supported thin film was strained to accommodate the misfit between the two materials. Such an approach enabled the stability and structure of interfaces between different materials to be derived. That the incommensurate materials are strained into coherency reduces substantially the computational expense: periodic boundary conditions (PBC) can be employed and the initial positions of the individual ions are based on the particular NCSL and are therefore predetermined. Conversely, there was no relaxation of the coherency by the formation of an array of dislocations, contrary to what is observed experimentally.[6] Moreover, Schnitker and Srolovitz investigated the errors introduced into the work of adhesion associated with such assumptions of coherency and found they increased rapidly with misfit and can be 'easily of the order of several tens of percent'.[7] The authors attributed such errors to the neglect of the elastic fields associated with misfit dislocations and to the variation in the number of bonds per unit interfacial area with misfit when coherency is assumed. Improved interface models must therefore account for the influence of dislocations within the lattice. Accordingly, to address such inadequacies of previous models, we have, in this present study, constructed thin film interfaces *via* the sequential deposition of ions onto the substrate surface. Moreover, we show that the method is capable of generating models representative of the structural evolution of misfit induced dislocations within supported thin films observed experimentally.[8] We also note that Dong *et al*. have employed a similar approach in which they predict the critical thickness of a thin film, above which dislocations nucleate, relaxing most of the misfit.[9] However, the authors employed a two-dimensional representation of the surface to reduce the computational expense.

In this present study we investigate a range of oxide–oxide interfaces associated with lattice misfits spanning −20 to +27% and focus on the structural modifications that may evolve within the thin film to help accommodate the lattice misfit. In addition we examine the influence that steps and buffer layers on the surface of the support material may have on the structure of the deposited thin film. Finally we investigate the deposition of mixed oxides on a support material.

## Methodology

The MARVIN code[10] was used to perform all the atomistic simulations presented in this study including energy minimisation and dynamics simulation. The code considers the crystal as a stack of ions periodic in two dimensions. The stack is subdivided into two regions: a region I, where all the ions are allowed to relax explicitly, and a region II, where the ions are all held fixed relative to each other. Region II is included to ensure that the long-range effects of the ions in the bulk of the crystal on the surface region are correctly represented. The top of region I is the free surface, onto which ions, comprising the thin film, are deposited thus creating the interface. To reduce the computational cost, region I for the support was two layers thick. It has been shown previously[8] that increasing the thickness of region I does not influence the structure of the thin film.

The reliability and quality of the simulation results are intimately dependent upon the potential models describing the materials under investigation. The interionic potentials used in this present study are, as is normally the case for metal oxides, based on the Born model of the ionic solid in which the ions interact *via* long-range Coulombic interactions and short-range, parameterised interactions. Potential parameters for all the ions considered in this study were taken from Lewis and Catlow.[11] In addition, a rigid ion model was used to reduce the computational expense.

## Deposition procedure

The construction of the thin film was achieved by successively depositing those ions comprising the thin film onto the surface of the support. In particular, the ions were introduced at a random position above the surface and moved vertically towards the surface until they were within 2.5 Å of the support or any previously deposited species. After this, energy minimisation and/or dynamics simulation was applied to the system, comprising the support and ions deposited, to direct the species into low energy positions. This procedure was repeated until the required thin film thickness was achieved. A more detailed account of the procedure has been given previously.[8]

The stability of each interface was characterised *via* the surface energy, which is given (following Gay and Rohl[10]), by:

$$\gamma_{(hkl)} = [E_{\text{total}}(hkl) - E_{\text{boundary}}(hkl) - nE_{\text{substrate}} - mE_{\text{film}}]/ 2A(hkl) \quad (1)$$

where $\gamma$ is the surface energy of the interface; $E_{\text{total}}$, the total energy of the interface; $E_{\text{boundary}}$, the boundary interaction energy; $E_{\text{substrate}}$ and $E_{\text{film}}$, the energy of the perfect crystal comprising the support and overlying thin film respectively; $n$ and $m$, the number of primitive unit cells within the support and overlying thin film respectively; $A$, the interfacial area and ($hkl$) the Miller indices defining the particular surface of the support.

A major limitation with molecular dynamics simulations is the timescale achievable, which is generally of the order of nanoseconds. However, by performing the simulations at elevated temperatures, typically 2100 K in this study, the surface diffusivity of the deposited ions are increased, enabling a more extensive exploration of the configurational space.

## Results

### CaO/MgO(100); 10 × 10 MgO(100) lattice

The first interface considered was the CaO/MgO(100), which is associated with a +13% misfit. We denote a positive misfit as referring to the situation in which the supported material has a larger lattice parameter compared with the substrate. Following the deposition procedure outlined above, CaO species were deposited onto a 10 × 10 MgO substrate until the desired thin film thickness was achieved. The '10 × 10' refers to the size of the simulation cell and corresponds to ten atoms or five MgO repeat units for each side of the supercell. Each layer within the periodic simulation cell therefore comprises 100 atoms (50 magnesium and 50 oxygen atoms).

Fig. 1(a)–(c) depict the interface structures after the deposition of 1.8, 2.9 and 3.9 equivalent CaO monolayers onto the MgO(100) surface respectively, while Table 1 presents the

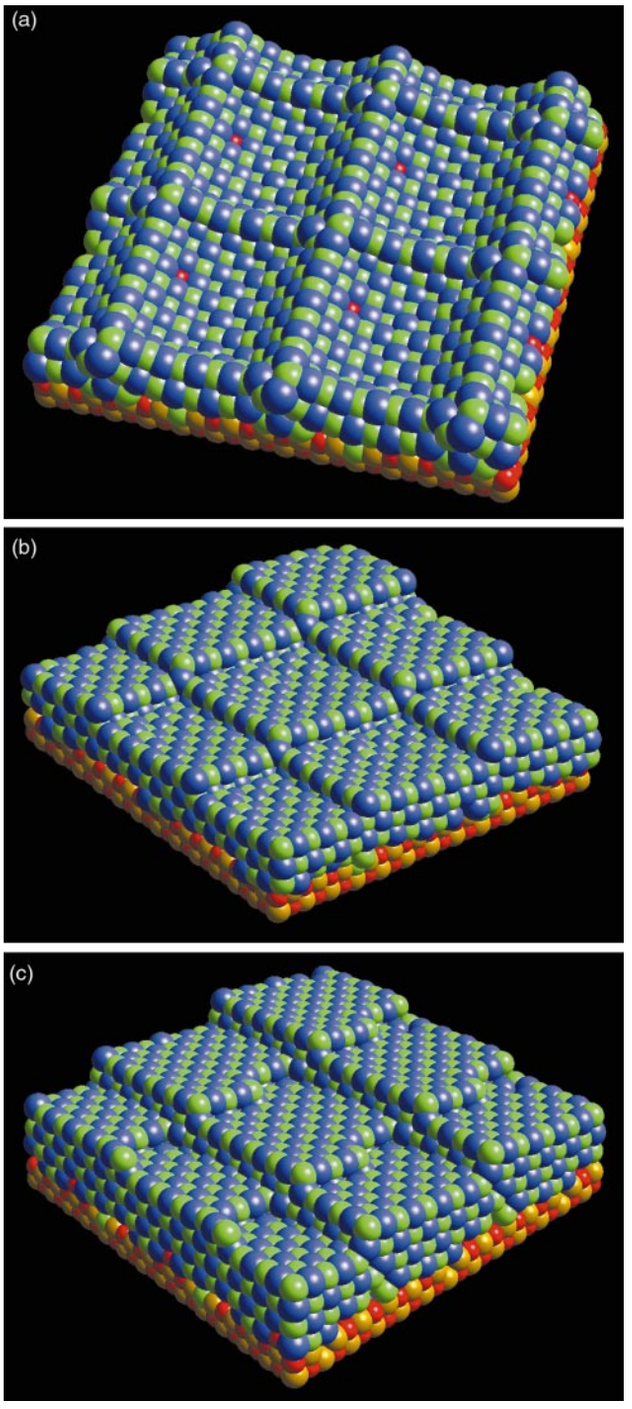


**Fig. 1** Representation of the CaO/MgO(100) system after the deposition of (a) 1.8, (b) 2.9 and (c) 3.9 equivalent CaO monolayers onto a 10 × 10 MgO(100) surface. Calcium is coloured blue, magnesium is yellow, oxygen (CaO) is green and oxygen (MgO) is red. For reasons of clarity, only two planes of the MgO support are shown (region I) whilst region II, which represents the bulk crystal and effectively extends to infinity, is not displayed.

**Table 1** Calculated surface energy, associated misfit, thin film thickness (monolayers), observed structure and reference to a pictorial representation of the structure for each of the oxide–oxide interface systems considered in this study

| System | Misfit (%) | Monolayers | Surface energy/J $m^{-2}$ | Thin film structure | Fig. |
|---|---|---|---|---|---|
| CaO/MgO(100) (10 × 10) | +13 | 1.8 | 2.00 | CaO(110) and CaO(100) | 1(a), 2 |
| | | 2.9 | 2.20 | Dislocations | 1(b) |
| | | 3.9 | 2.31 | Dislocations + slip | 1(c), 3 |
| CaO/MgO(100) (12 × 12) | +13 | 1.5 | 1.85 | CaO(110) and CaO(100) | 4(a) |
| | | 1.8 | 1.98 | CaO(310), CaO(100) | 4(b), 5 |
| | | 3.6 | 1.54 | Rotation (5°) + dislocation | 4(c) |
| CaO/MgO(510) | +13 | 1.3 | 2.30 | CaO 'strips' | 6(a), 6(b) |
| | | 2.5 | 2.48 | Dislocations | 7 |
| | | 3.8 | 1.99 | Rotation (6°) | 8(a), 8(b) |
| MgO/SrO(100) | −20 | 0.52 | 1.16 | 'Amorphous' | — |
| | | 1.06 | 1.31 | 'Amorphous' | — |
| | | 2.68 | 1.86 | 'Amorphous' | — |
| SrO/MgO(100) | +20 | — | — | 'Amorphous' | — |
| BaO/MgO(100) | +27 | 2.63 | 1.85 | Rotation (14°) | — |
| | | >2.63 | — | 'Amorphous' | — |
| SrO/CaO/MgO(100) | +13 (CaO) | 1.8 (CaO) | 2.50 | Cubic + pseudo-hexagonal (CaO) | 9(a)–(c) |
| | +20 (SrO) | 1.8 (SrO) | | Pseudo hexagonal (SrO) | |
| $Ba_{0.5}Ca_{0.5}O$/SrO(100) | 'Zero ?' | 0.78 | 0.88 | Pseudomorphic growth: $Ba_{0.5}Ca_{0.5}O$(100) | — |
| | | 1.58 | 1.02 | Pseudomorphic growth: $Ba_{0.5}Ca_{0.5}O$(100) | — |
| | | 2.00 | 0.93 | Pseudomorphic growth: $Ba_{0.5}Ca_{0.5}O$(100) | — |
| | | 3.58 | 1.26 | Pseudomorphic growth: $Ba_{0.5}Ca_{0.5}O$(100) | — |
| | | 4.00 | 0.82 | Pseudomorphic growth: $Ba_{0.5}Ca_{0.5}O$(100) | 10 |

calculated surface energies of these interfaces. To aid interpretation of the interfaces, the structures presented depict more than the primitive (10 × 10) simulation cell. In addition, the structures presented do not represent the 'correct' ionic radii.

We now look in more detail at the structural features of the thin film interfaces.

For 1.8 equivalent CaO monolayers deposited [Fig. 1(a)], the CaO exhibits the rocksalt structure which appears to expose principally the CaO(100) surface at the interface. To aid interpretation, Fig. 2 depicts a schematic of this interface which illustrates more clearly the exposure of both the CaO(100) and (110) planes at the interfacial region. The latter rationalises the 'peaks' that can be observed on the surface of the CaO thin film [Fig. 1(a)]. The figure also demonstrates that the Ca and O species at the interfacial plane maintain almost perfect registry with their respective O and Mg counter ions of the support for both the CaO(100) and CaO(110) regions.

That the CaO exposes both the (110) and (100) surfaces at the interface can be rationalised by considering the lattice misfit between the CaO and MgO. For example, the exposure of the CaO(100) surface at the interface is associated with a +13% misfit, and to maintain registry of the Ca and O ions with their respective counter ions of the underlying MgO support, the CaO must be in compression. Conversely, the CaO is in tension while exposing the (110) surface (−22% misfit) at the interface. The subsequent ionic relaxation enables the strain energy, generated within the CaO thin film under opposing conditions of tension and compression, to be diminished. The intersection of the CaO(110) with the CaO(100) is a grain-boundary.

After the deposition of 2.9 equivalent monolayers [Fig. 1(b)], orthogonal steps are present on the surface of the CaO thin film, which indicate the presence of a periodic array of dislocations within the CaO thin film. The formation of misfit induced dislocations has been well documented in the literature. In particular, Springholz used scanning tunneling microscopy to image subsurface dislocations in lattice mismatched thin film interfaces.[12] The author demonstrated that the local lattice distortion present around the interfacial dislocations give rise to pronounced deformations (steps) on the surface of the thin film providing direct experimental support for our model.

The driving force for dislocation formation is to reduce the strain energy generated within the thin film, which arises from the misfit between the two materials. In particular, the structural modification of the CaO can be described as the periodic removal of one CaO plane from every ten. The misfit can thus be calculated to be *ca.* +3%, in contrast to the original +13%, based on nine CaO planes lattice matched with ten planes of the underlying MgO support.

The dislocations [Fig. 1(b)] are retained within the thin film after 3.9 equivalent monolayers have been deposited onto the surface [Fig. 1(c)]. However, in one direction the steps are no longer monatomic, rather they are almost diatomic. A side view of the interface (Fig. 3) demonstrates that a further dislocation is starting to form. The dislocation is not complete, rather the structure can be described as a 'slip' of the CaO lattice which reduces further the misfit. However, although the misfit for 3.9 monolayers is effectively lower than that for either 1.8 or 2.9 monolayers, the calculated surface energy of this interface is higher, reflecting the increase in the strain energy, generated

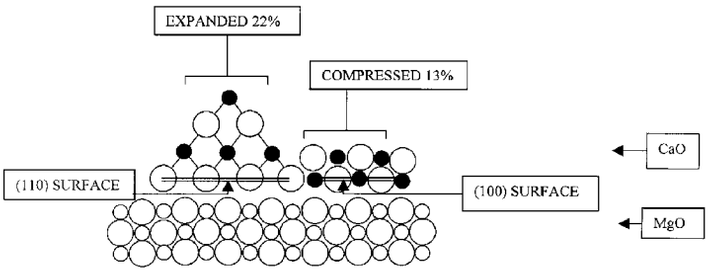


**Fig. 2** Schematic of the structure presented in Fig. 1(a). Oxygen species are represented by the large hollow circles, calcium, the small filled circles and magnesium the small hollow circles.

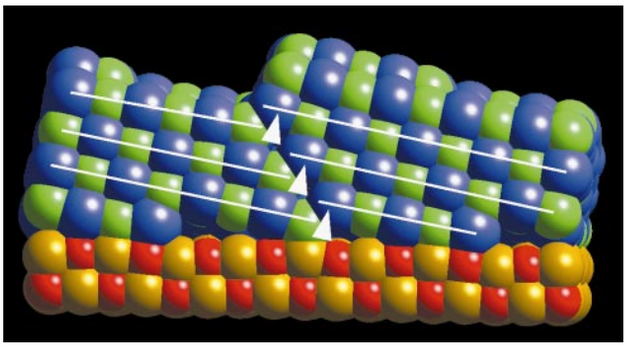

**Fig. 3** An enlarged side view of Fig. 1(c) illustrating the lattice slip of the CaO lattice (arrows). Notation as in Fig. 1.

within the lattice, with deposition level for incommensurate systems.

The construction of interfacial models of incommensurate systems requires large supercells, which must also be small enough to be accommodated within the computational resources available. The inclusion of periodic boundary conditions reduces considerably the computational expense enabling incommensurate systems to be considered using atomistic simulation techniques. However, such boundary conditions will firstly influence the structure of the thin film and secondly prohibit certain structural features that are larger than the simulation cell from forming, such as misfit induced grain boundaries. Experimentally, there exists a wealth on information on misfit induced dislocations within incommensurate oxide–oxide interface systems. For example, Ramesh *et al.* studied the epitaxial relationship between Y–Ba–Cu–O (YBCO) thin films grown on single crystal MgO(100).[2] A HREM image of the substrate–thin film interface showed that the lattice misfit was accommodated by a periodic array of interfacial dislocations. The periodicity corresponds to the matching of three YBCO(110) planes with four (100) planes of the MgO lattice. To model such a configuration a $4\times4$ primitive MgO(100) unit cell would be required, while in this present study we consider primitive unit cells which are an order of magnitude larger with respect to the surface area. Consequently we suggest such cells are sufficiently large for the results to provide useful information on structural modifications arising from the misfit between two incommensurate lattices. In the following section we examine the influence of increasing the primitive cell size.

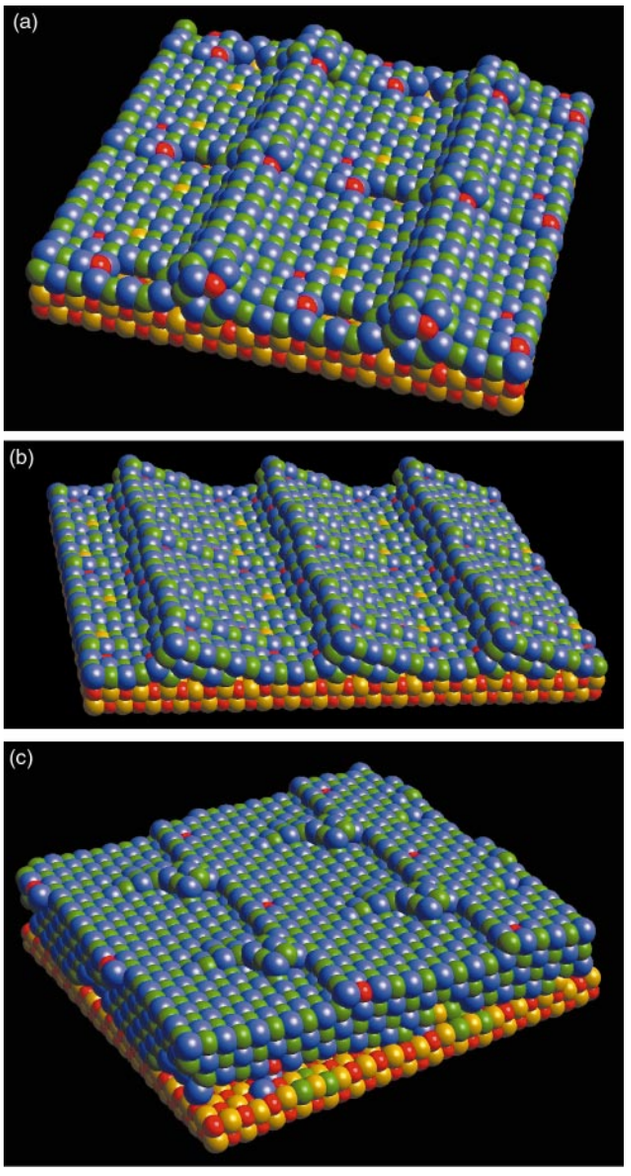


**Fig. 4** Representation of the CaO/MgO(100) system after the deposition of (a) 1.5, (b) 1.8 and (c) 3.6 equivalent CaO monolayers onto a $12\times12$ MgO(100) surface. Notation as in Fig. 1.

### CaO/MgO(100); $12\times12$ MgO(100) lattice

In this section, the primitive cell size for the CaO/MgO(100) system is increased from 441 to 635 Å$^2$ which is achieved by depositing the CaO species onto a $12\times12$ MgO(100) lattice.

Fig. 4(a)–(c) depict the interface structures after the deposition of 1.5, 1.8 and 3.6 equivalent monolayers onto the MgO(100) surface, respectively.

For 1.5 equivalent monolayers, the CaO thin film exhibits similar structural characteristics to those observed previously using the $10\times10$ MgO(100) support. In particular, the CaO exposes both the CaO(100) and (110) surfaces at the interface with Ca and O species lying directly above their respective O and Mg counter ions of the MgO support.

Upon increasing the thin film thickness to 1.8 equivalent monolayers, the CaO can be seen to expose both the CaO(310) and (100) surfaces at the interface [Fig. 4(b)]. A schematic, to aid the interpretation of this structure, is presented in Fig. 5. The CaO(310)/MgO(100) is associated with a $-10\%$ misfit, which compensates for the $+13\%$ misfit associated with the CaO(100)/MgO(100) regions. Close inspection of Fig. 4(b) reveals a degree of rumpling on the surface of the CaO thin film

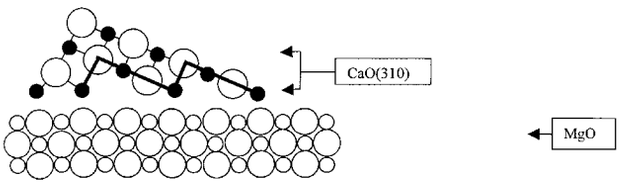


**Fig. 5** Schematic of the structure presented Fig. 4(b). Oxygen species are represented by the large hollow circles, calcium, the small filled circles and magnesium the small hollow circles.

which facilitates a further reduction in the lattice misfit and improves the registry between counter ions across the interface.

After the deposition of 3.6 equivalent monolayers, the CaO thin film is observed to have rotated by *ca.* 5° with respect to the underlying MgO support [Fig. 4(c)] while exposing only the (100) surface at the interface. In addition, dislocations have formed within the CaO, which are indicated by the monatomic steps present on the surface of the CaO thin film. It is interesting to note that the dislocation lies along the MgO[100] direction.

Consequently, as the CaO thin film is rotated with respect to the MgO support, the steps on the CaO surface contain kinks. Moreover, as the ions at the kink sites exhibit low coordinative saturation, they act as nucleation centres for the further growth of the CaO lattice. Indeed, Fig. 4 shows small CaO clusters have been adsorbed in these regions.

Several experimental studies provide evidence for the overlying oxide film rotating with respect to the support material. For example a study by Chern on the MgO/$SrTiO_3$(001) system[13] suggests that the MgO overlayers are rotated by 45° relative to the SrO terminated $SrTiO_3$(001) support which is associated with a +7.8% misfit. Cotter *et al.* also proposed, a 45° rotation of the BaO(100) with respect to the MgO(100) support in the BaO/MgO(100) system[14] thereby facilitating a reduction in the lattice misfit from 27% for pseudomorphic growth to *ca.* 8% for the rotated configuration. In addition Hwang *et al.* employed a NCSL approach, to help explain the various orientations of $YBa_2Cu_3O_{7-x}$ grains observed when supported on MgO(100) substrates,[15] suggesting that the rotated configurations are associated with low lattice misfits. Applying a simplified (2-D) NCSL approach to the CaO/MgO(100) system [Fig. 4(c)], suggests that the rotation of the CaO facilitates a reduction in the lattice misfit from +13% to *ca.* +5%. This value is reduced further when one includes, in addition, the influence of the dislocation within the CaO thin film.

It is interesting to note that in contrast to the '12 × 12' CaO/MgO system, the CaO thin film in the '10 × 10' CaO/MgO did not expose the CaO(310) surface. We suggest the '10 × 10' system is too small to accommodate regions of both (310) and (100). Similarly, the structure presented in Fig. 4(c) where the CaO is rotated with respect to the underlying MgO is also larger than can be accommodated using a 10 × 10 primitive unit cell. Such observations demonstrate that small primitive unit cell sizes are inadequate to model certain structural features. Inevitably, the primitive unit cell size considered in this present study will preclude certain structural features from being identified. However, the simulation does provide useful insights into the structural modifications that the overlying thin film may accommodate to reduce the misfit. These include as the exposure of different CaO surfaces, the formation of dislocations and lattice rotations. Clearly, exposure to increased computational resources will enable the identification of additional structural features leading to a greater understanding of epitaxial processes.

## CaO/MgO(510)

Experimentally, surfaces are rarely perfect, *i.e.* monatomically flat, and depending on their preparative method, will include a degree of surface roughness[16] which may include, for example surface steps, defect as well as contaminant ions and adsorbed surface species.[17] Moreover, such surface irregularities play an important role in many processes such as chemical reactivity, sorption of ions, adhesion and surface diffusion and are likely therefore to influence considerably the structure of the thin film generated *via* deposition methods. Clearly, such features must be included if one is to construct more realistic simulation models. Accordingly, in this section we investigate the influence that surface steps, present on the MgO support material, may have on the structure of the CaO thin film deposited thereon. In particular, following the procedure outlined above, CaO species were deposited sequentially onto an MgO(510) surface, which comprises a periodic array of monatomic steps on the surface.

After 1.3 equivalent monolayers of CaO have been deposited, orthogonal CaO 'strips' are observed on the MgO support [Fig. 6(a)]. A side view of this structure, [Fig. 6(b)], shows that the deposited CaO reduces the atomic sharpness of the steps on the MgO surface, the two arrows on the figure

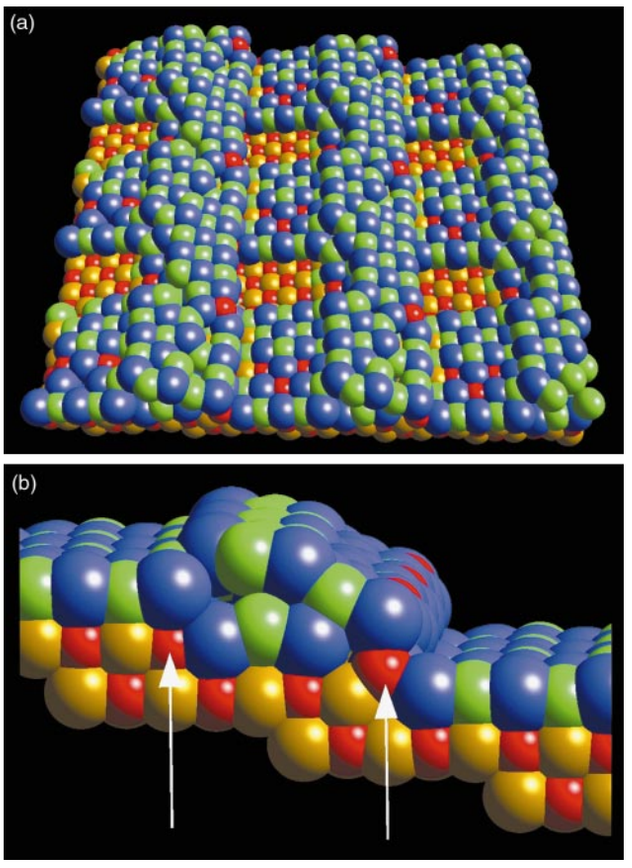


**Fig. 6** Representation of the CaO/MgO(510) system after the deposition of 1.3 equivalent CaO monolayers; (a) projection looking down on the surface and (b) a side view of the interface illustrating the position of the steps on the MgO surface (arrows). Notation as in Fig. 1.

indicate the original positions of the monatomic steps. Such behaviour, is not however unexpected since surface steps are essentially defects which are less stable compared with a perfect surface.[16]

After 2.5 equivalent monolayers have been deposited, steps on the surface of the CaO thin film are evident (Fig. 7). We suggest however, that the surface steps on the CaO do not reflect an extension of the surface steps on the surface of the MgO support since, first, orthogonal steps are present on the CaO and second, the interstep distance on the CaO surface is much larger compared with the underlying MgO. Rather, they indicate the presence of dislocations within the CaO thin film.

Finally after the deposition of 3.8 equivalent monolayers,

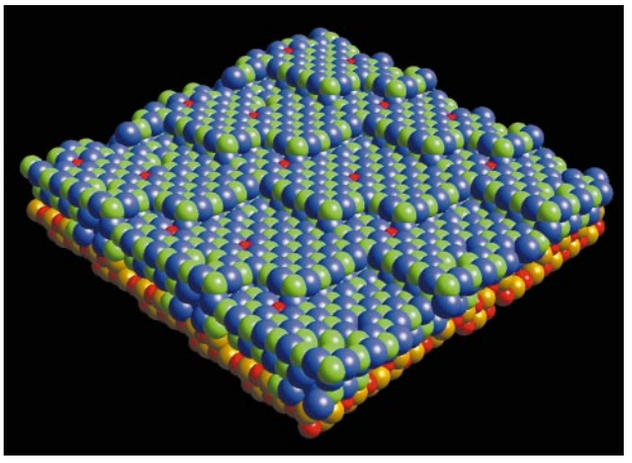

**Fig. 7** Representation of the CaO/MgO(510) system after the deposition of 2.5 equivalent monolayers. Notation as in Fig. 1.

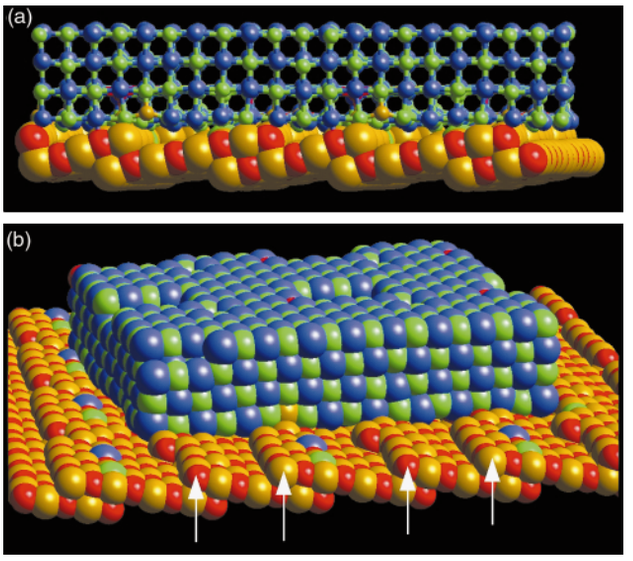


**Fig. 8** Representation of the CaO/MgO(510) system after the deposition of 3.8 equivalent monolayers; (a) side view of the interface and (b) perspective view depicting a part of the CaO thin film to illustrate more clearly the rotation of the CaO thin film with respect to the MgO support. Notation as in Fig. 1.

steps at the surface of the CaO are no longer present [Fig. 8(a), (b)] which suggests that the dislocations within the CaO thin film have been annealed out of the structure during the dynamics simulation. Moreover, the CaO has undergone a rotation of *ca.* 6° about an axis normal to the MgO surface. The misfit for this rotated structure can be estimated, using a NCSL theory as *ca.* +1% parallel and *ca.* +3% perpendicular to the MgO surface steps, respectively. Clearly, the driving force for such a structural transformation is a reduction in the strain energy generated within the lattice.

Ironically, much experimental work is focussed on reducing or indeed eliminating such surface irregularities which reduces the complexity of the simulation models required.

### Supported oxides with high misfit

In this section we extend our study to include interfaces with much higher lattice misfits. In particular, three interfaces are considered: MgO/SrO(100), SrO/MgO(100) and BaO/MgO(100) which are associated with lattice misfits of −20, +20 and +27%, respectively.

For the MgO/SrO(100) system (−20% misfit), after the deposition of 0.3 equivalent monolayers, MgO clusters adopting a cubic-type structure formed on the surface of the SrO(100) support. In addition, certain MgO clusters were observed to be rotated about an axis perpendicular to the SrO surface. In all cases the Mg and O species maintained registry with their corresponding O and Sr counter ions of the SrO support. At deposition levels of 0.5 monolayers a proportion of the MgO clusters exhibited pseudo-hexagonal type configurations in addition to cubic-type structure, while at higher deposition levels, the structure of the MgO appeared amorphous.

In an attempt to obtain a more coherent structure, dynamics simulation was performed on an MgO/SrO(100) system with an MgO coverage of 2.7 equivalent monolayers at various temperatures ranging from 800 to 2100 K for a total of 2.5 ns. While the uppermost (surface) MgO layer exhibited a pseudo-hexagonal type structure, the structure of the MgO nearer the interface remained amorphous with no discernible evidence of any discrete MgO layers.

The next system considered was the SrO/MgO(100) interface (+20% misfit), which is the inverted analogue of the previous system. Inspection of the resulting thin film interface structures again revealed no discernible crystallinity for the supported SrO thin film.

Finally, for the BaO/MgO(100) system, a crystalline thin film interface was obtained for 2.63 equivalent BaO monolayers deposited onto the MgO surface. Inspection of the interface structure revealed that the BaO thin film was rotated by *ca.* 14° relative to the MgO support with incomplete filling of the interfacial BaO layer. Moreover, the interplanar spacing at the interface ranged from *ca.* 3.5 to 4.0 Å which is considerably higher compared to the Ba–O distances of 2.75 Å found in pure BaO, reflecting a weak interfacial adhesion. Further deposition of BaO species resulted in amorphous type interface structures.

An experimental study by Mestl *et al.* on the catalytic properties of the BaO/MgO system suggests that when supported on MgO, the BaO exhibits the rocksalt structure, which is 'ill defined crystallographically' and contains lattice defects.[18]

Thus far we have investigated the profound influence the lattice misfit may have on the structure of supported thin films. In the following section we consider the possibility of exercising some control over such structures. For example, is it possible to reduce or indeed eliminate the formation of misfit induced dislocation arrays within supported thin films? Two mechanisms for achieving this objective are considered, the first involves the inclusion of buffer layers, while for the second, dopant ions are introduced into the thin film with the aim of modifying the lattice parameter to be commensurate with that of the support material.

### Buffer layers; the SrO/CaO/MgO(100) interface

Much experimental work has focussed on the effect the lattice misfit has on the structure of thin film interfaces. In particular the misfit has been shown to be accommodated by the presence of defects such as vacancies, grain-boundaries and dislocation arrays, the latter clearly identified in this present study. In many cases, such misfit induced structural changes can have severe implications for the material properties and hence the particular application of the material. For example, misfit induced dislocations within supported superconductors can result in poor electrical properties.[19] One solution to this problem has been the introduction of buffer layers between the substrate and the supported thin film,[20] the buffer layer accommodating much of the misfit strain and resultant defects and dislocations so damaging to the electrical properties of the thin film superconductor.

Simulation techniques have also been employed to explore the influence of introducing buffer layers. In particular, a theoretical study by Kubo *et al.* showed that by introducing buffer layers within the $YBa_2Cu_3O_{7-x}/SrTiO_3$ interface, a system with no observable stress could be constructed.[21] In this present study we explore the possibility of whether the inclusion of a buffer layer could improve the crystallinity of oxide–oxide interfaces with high associated lattice misfits. In particular we consider the SrO/MgO(100) interface for which no observable crystallinity could be observed.

In the previous section, SrO species, when deposited onto an MgO(100) substrate, resulted in the formation of an 'amorphous' SrO thin film. To determine whether a coherent SrO thin film could be grown onto an MgO(100) substrate, a thin film of CaO was deposited onto the MgO(100) prior to the deposition of the SrO. A CaO buffer layer was chosen as the CaO/MgO(100) interface is associated with a smaller lattice misfit compared with the SrO/MgO(100) system. Moreover, thin films of CaO were observed (above) to form coherent structures on the MgO(100) support. Accordingly, an SrO/CaO/MgO(100) interface was constructed by depositing 1.8 equivalent monolayers of the CaO 'buffer layer', followed by 1.8 equivalent monolayers of SrO. Dynamics simulation was then applied to the resulting structure for 2.74 ns at 1200 K.

In contrast to the 'amorphous' structure observed for the SrO/MgO(100) system, the SrO/CaO/MgO(100) system was observed to be crystalline. Fig. 9(a) shows a view perpendicular to the surface of the thin film and includes, for reasons of clarity, only the interfacial layer and the underlying MgO(001) support. This interfacial layer (buffer layer) does not however comprise solely CaO, rather 22% of the cations in this plane are Sr and 3% are Mg, which have migrated from adjacent planes. The structure of the interfacial plane is mainly cubic, but also comprises regions, which appear to have a 'pseudo-hexagonal' type configuration. Fig. 9(b) shows the same projection as Fig. 9(a) but includes all the CaO and SrO layers, while Fig. 9(c) presents a perspective view of the thin film. The structure is coherent, however, the SrO overlayers adopt a pseudo-hexagonal as opposed to cubic type configuration. Such a structure was observed in a previous study on the CaO/SrO(100) system[8] which suggests that a transformation from a cubic to a pseudo-hexagonal type configuration is associated with a change in the interfacial area and thereby provides an additional mechanism for reducing the interfacial misfit.

The calculation suggests that by depositing a CaO buffer layer, which has a lower associated lattice misfit, prior to depositing the SrO, affords a way of constructing a more coherent SrO thin film.

Owing to the random nature of the deposition procedure, repeating the procedure for constructing this SrO/CaO/MgO(100) system is likely to result in a range of different interfacial configurations. Moreover, many more parameters could be changed, including for example, buffer thickness, multiple buffers, and the nature of the MgO support. Such studies will clearly improve our current understanding of the mechanisms by which buffer layers are able to influence and ultimately improve the structure of supported thin films.

In the following section we consider a slightly different approach for accommodating the lattice misfit, in which dopant ions are introduced into the supported thin film to effect a change in the lattice parameter of the thin film.

### Mixed oxides; the $Ba_{0.5}Ca_{0.5}O$/SrO(100) interface

The lattice parameter of a material may be modified *via* the introduction of dopant ions into the lattice, for example see refs. 22 and 23. Presumably, by introducing a particular concentration of dopant ions into the supported thin film, it may be possible to modify the lattice parameter to be commensurate with that of the substrate.

In a previous study it was found that the +7% misfit associated with the BaO/SrO(100) interface was accommodated by the formation of a periodic array of dislocations within the BaO thin film.[8] Conversely, for the CaO/SrO(100) system, which is associated with a −7% misfit, 'cracks' within the CaO thin film were observed. To attempt to reduce the misfit between the support material and the overlying thin film, a mixed oxide film comprising equal quantities of BaO and CaO was deposited onto an SrO(001) surface, *i.e.* $Ba_{0.5}Ca_{0.5}O$/SrO(001). The +7% misfit associated with the BaO/SrO system would therefore presumably be accommodated by the subsequent change in the BaO lattice parameter when Ca species are introduced into the lattice.

To effect the deposition of a $Ba_{0.5}Ca_{0.5}O$ thin film onto an SrO(100) support, the deposition process was slightly modified such that BaO and CaO were deposited alternately onto the SrO(100) support. This procedure was continued until the equivalent of four monolayers had been deposited. The surface energies of five interfaces with $Ba_{0.5}Ca_{0.5}O$ coverages ranging from 1–4 equivalent monolayers are presented in Table 1, while Table 2 reports the average bond distances and cation distributions within each plane for the system comprising four $Ba_{0.5}Ca_{0.5}O$ planes (Fig. 10).

Analysis of the interface structures revealed that the

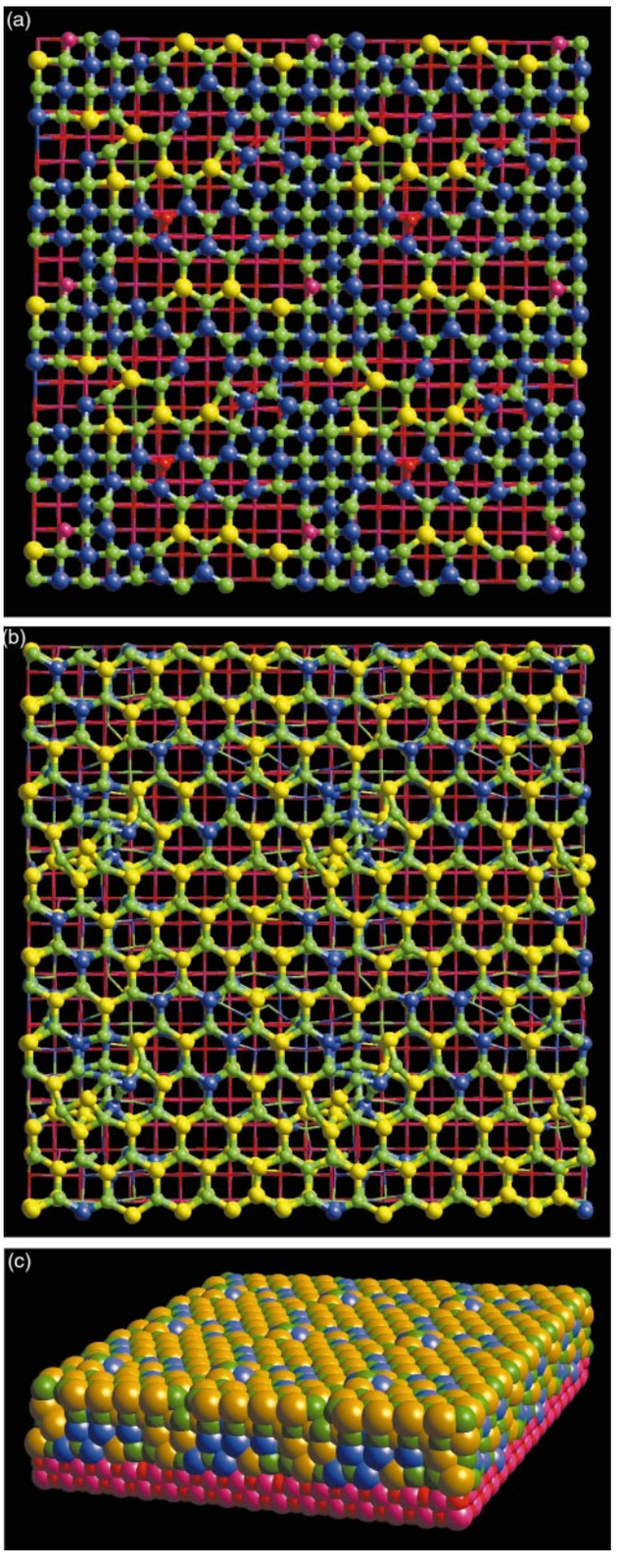


**Fig. 9** Representation of the SrO/CaO/MgO(100) system; (a) a projection illustrating only the interfacial (CaO buffer layer), (b) a projection depicting the whole system and (c) filled sphere, perspective view of the interface. For (a) and (b), the MgO support is represented by a stick model, while the thin film is represented by a ball and stick model. Magnesium ions are coloured purple, calcium is blue, strontium is yellow, oxygen (MgO) is red and oxygen (CaO, SrO) is green.

$Ba_{0.5}Ca_{0.5}O$ thin films were all coherent with respect to the underlying SrO(100) support with no evidence of dislocations within the thin film. Moreover, the $Ba_{0.5}Ca_{0.5}O$ thin film exposed exclusively the (100) surface at the interface with

**Table 2** Cation distributions and cation–oxygen bond distances for the $Ba_{0.5}Ca_{0.5}O/SrO(100)$ interface with four equivalent $Ba_{0.5}Ca_{0.5}O$ monolayers deposited onto the SrO(100) surface (Fig. 10). Plane 1 refers to the surface plane of the $Ba_{0.5}Ca_{0.5}O$ thin film, plane 4, the interfacial $Ba_{0.5}Ca_{0.5}O$ plane and plane 5 the interfacial SrO plane. The cation–oxygen bond distances for pure BaO,CaO and SrO are given as a comparison

| Plane | Ba(%) | Ca(%) | Sr(%) | Ba–O/Å | Ca–O/Å | Sr–O/Å |
|---|---|---|---|---|---|---|
| 1 | 58 | 42 | 0 | 2.60 | 2.35 | — |
| 2 | 42 | 56 | 2 | 2.65 | 2.45 | 2.59 |
| 3 | 48 | 52 | 0 | 2.67 | 2.42 | — |
| 4 | 48 | 44 | 8 | 2.65 | 2.50 | 2.57 |
| 5 | 4 | 6 | 90 | 2.67 | 2.53 | 2.57 |
| 6 | 0 | 0 | 100 | — | — | 2.57 |
| Bulk | | | | 2.75 | 2.38 | 2.57 |

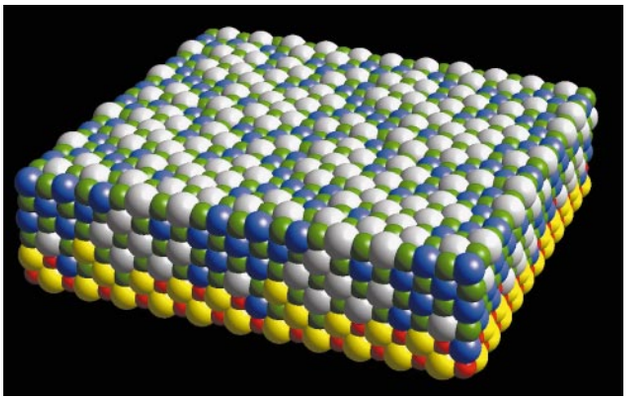

**Fig. 10** Representation of the $Ba_{0.5}Ca_{0.5}O/SrO(100)$ interface with 4 equivalent $Ba_{0.5}Ca_{0.5}O$ monolayers on the SrO(100) support. Barium is coloured white, calcium is blue, strontium is yellow, oxygen (SrO) is red and oxygen ($Ba_{0.5}Ca_{0.5}O$) is green.

cations and anions of the thin film lying directly above their respective counter ions of the SrO support. Inspection of the structure shown in Fig. 10 reveals an even distribution of Ba and Ca species in each plane as one might expect: regions comprising exclusively CaO or BaO are likely to be strained. Table 2 also suggests that to facilitate pseudomorphic growth of the thin film with respect to the SrO support, the average Ba–O and Ca–O bond distances are modified by *ca.* $-0.11$ and $+0.05$ Å respectively. That the Ba–O distances are modified to a much greater degree compared with Ca–O reflects the lower energy associated with straining a BaO lattice compared with a CaO lattice.

The very simple model system we have considered here suggests that the misfit between two incommensurate materials may be modified by introducing dopant ions within the thin film. Such an approach will, in future studies, be extended to investigate more commercially important systems, which may include, for example, Zr doped $CeO_2/Al_2O_3$ which is an important component of the three-way automobile exhaust catalyst.

## Conclusions

In the initial stages of growth, the configuration of a supported thin film is governed by the ion–ion interactions across the interface, consequently, the thin film will be constrained into a particular crystallographic relationship with the support material.[24] Moreover, as the deposition continues, so the strain energy generated within the thin film increases until, at a particular thickness, it becomes energetically favourable to relieve this strain energy *via* a structural modification(s) of the thin film. However, although such structural changes may be thermodynamically favourable, the kinetic pathways for the evolution of such structural modifications must also be surmountable. Experimental observations on supported thin films confirm that such structural changes occur at a particular 'critical thickness'. Previous simulation models have proved inadequate in reproducing either misfit-induced dislocations or addressing the kinetic aspects of thin film growth. Accordingly, in this present study we have been able to accommodate both issues. In particular we have considered an alternative approach of constructing the thin film *via* the sequential deposition of individual ions onto the substrate surface. Moreover, the method facilitates the evolution (*via* dynamics simulation) of structural modifications of the thin film: for the CaO/MgO(100) system, the CaO was observed to expose the (100), (110) and (310) surfaces at the interface, while at higher deposition levels the formation of orthogonal dislocations, including lattice slip, was observed within the CaO thin film together with rotations of the CaO with respect to the underlying support. In each case the structural modifications related to a reduction in the strain energy, generated within the thin film as a consequence of the misfit between the two incommensurate materials.

In the second part of this study we have explored briefly how one may exercise a degree of control over the influence of the lattice misfit and its implications for the structure and consequently the chemical and physical properties of the thin film. First, by including a CaO buffer layer within the SrO/MgO(100) interface a coherent SrO thin film structure was derived, in contrast to the amorphous structure observed without a buffer. Second, for the BaO/SrO(100) system, by introducing calcium ions into the BaO thin film, the lattice parameter was modified sufficiently to ensure pseudomorphic growth on the support material, in contrast to the dislocations observed for the undoped BaO/SrO(100) system.

## References


1 G. C. Bond, S. Flamerz and R. Shukri, *Faraday Discuss., Chem. Soc.*, 1989, **87**, 65.
2 R. Ramesh, D. Hwang, T. S. Ravi, A. Inam, J. B. Barner, L. Nazar, S. W. Chan, C. Y. Chen, B. Dutta, T. Venkatesan and X. D. Wu, *Appl. Phys. Lett.*, 1990, **56**, 2243.
3 H. Grimmer, W. Bollmann and D. H. Warrington, *Acta Crystallogr., Sect. A*, 1974, **30**, 197.
4 R. W. Balluffi, A. Brokman and A. H. King, *Acta Metall.*, 1982, **30**, 1453.
5 T. X. T. Sayle, C. R. A. Catlow, D. C. Sayle, S. C. Parker and J. H. Harding, *Philos. Mag. A*, 1993, **68**, 565.
6 S. C. Jain, A. H. Harker and R. A. Cowley, *Philos. Mag. A*, 1997, **75**, 1461.
7 J. Schnitker and D. J. Srolovitz, *Modell. Simul. Mater. Sci. Eng.*, 1998, **6**, 153.
8 D. C. Sayle, *J. Mater. Chem.*, 1999, **9**, 607.
9 L. Dong, J. Schnitker, R. W. Smith and D. J. Srolovitz, *J. Appl. Phys.*, 1998, **83**, 217.
10 D. H. Gay and A. L. Rohl, *J. Chem. Soc., Faraday Trans.*, 1995, **91**, 925.
11 G. V. Lewis and C. R. A. Catlow, *J. Phys. C: Solid State Phys.*, 1985, **18**, 1149.
12 G. Springholz, *Appl. Surf. Sci.*, 1997, **112**, 12.
13 G. Chern, *Surf. Sci.*, 1997, **387**, 183.
14 M. Cotter, S. Campbell, R. G. Egdell and W. C. Mackrodt, *Surf. Sci.*, 1988, **197**, 208; M. Cotter, S. Campbell, L. L. Cao, R. G. Egdell and W. C. Mackrodt, *Surf. Sci.*, 1989, **208**, 267.

15 D. M. Hwang, T. S. Ravi, R. Ramesh, S. W. Chan, C. Y. Chen and L. Nazar, *Appl. Phys. Lett.*, 1990, **57**, 1690.
16 J. Goniakowski and C. Noguera, *Surf. Sci.*, 1995, **340**, 191.
17 N. H. de Leeuw, G. W. Watson and S. C. Parker, *J. Phys. Chem.*, 1995, **99**, 17219.
18 G. Mestl, M. P. Rosynek and J. H. Lunsford, *J. Phys. Chem. B*, 1997, **101**, 9321.
19 D. Dimos, P. Chaudhari and J. Mannhart, *Phys. Rev. B*, 1990, **41**, 4038.
20 O. Eibl, H. E. Hoenig, J.-M. Triscone, O. Fischer, L. Antognazza and O. Brunner, *Physica C*, 1990, **172**, 365; O. Eibl, H. E. Hoenig, J.-M. Triscone, O. Fischer, L. Antognazza and O. Brunner, *Physica C*, 1990, **172**, 373.
21 M. Kubo, Y. Oumi, R. Miura, A. Stirling, A. Miyamoto, M. Kawasaki, M. Yoshimoto and H. Koinuma, *Phys. Rev. B: Condens. Matter*, 1997, **56**, 13 535.
22 L. Minervini, M. O. Zacate and R. W. Grimes, *Solid State Ionics*, 1999, **116**, 339.
23 G. Balducci, J. Kaspar, Paolo Fornasiero, M. Graziani, M. S. Islam and J. D. Gale, *J. Phys. Chem. B*, 1997, **101**, 1750.
24 A. L. Shluger, A. L. Rohl and D. H. Gay, *Phys. Rev. B: Condens. Matter*, 1995, **51**, 13 631; A. L. Shluger, A. L. Rohl and D. H. Gay, *J. Vac. Sci. Technol. B*, 1995, **13**, 1190.

*Paper 9/05333F*